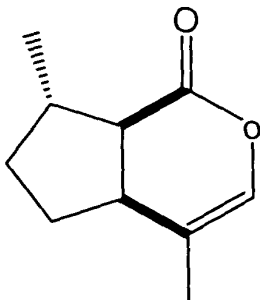
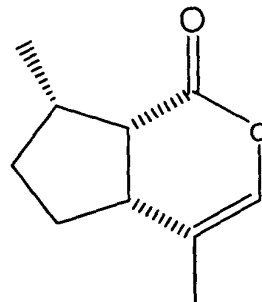


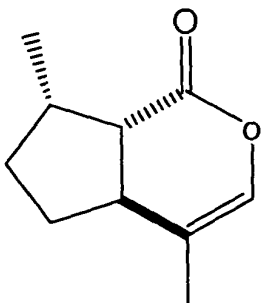
Figure 1 Structures of (7S)-nepetalactones



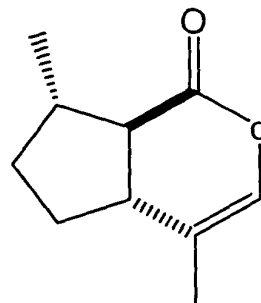
(4aS,7S,7aR) nepetalactone
(*cis,trans*-nepetalactone)



(4aR,7S,7aS) nepetalactone
(*cis,cis*-nepetalactone)



(4aS,7S,7aS) nepetalactone
(*trans,cis*-nepetalactone)



(4aR,7S,7aR) nepetalactone
(*trans,trans*-nepetalactone)

Figure 2 Total ion chromatograms from GC-MS analysis of fractionally distilled catmint oil before (A) and after (B) hydrogenation.

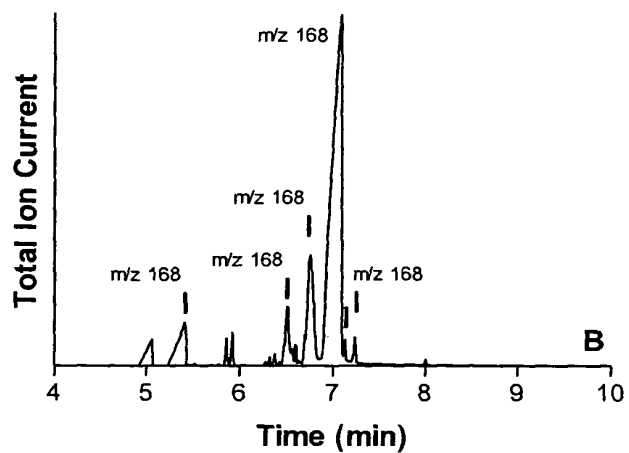
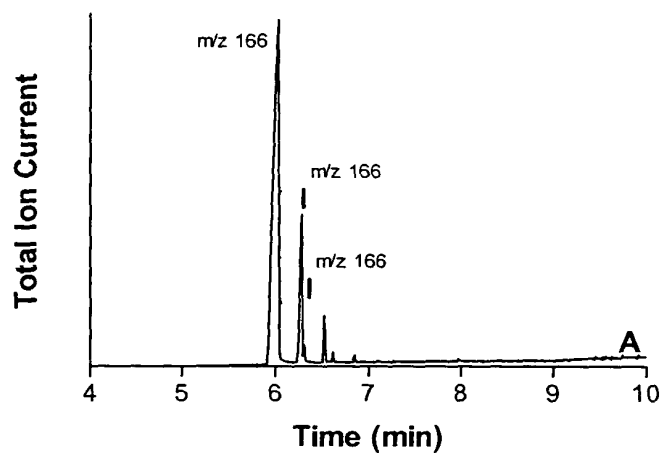
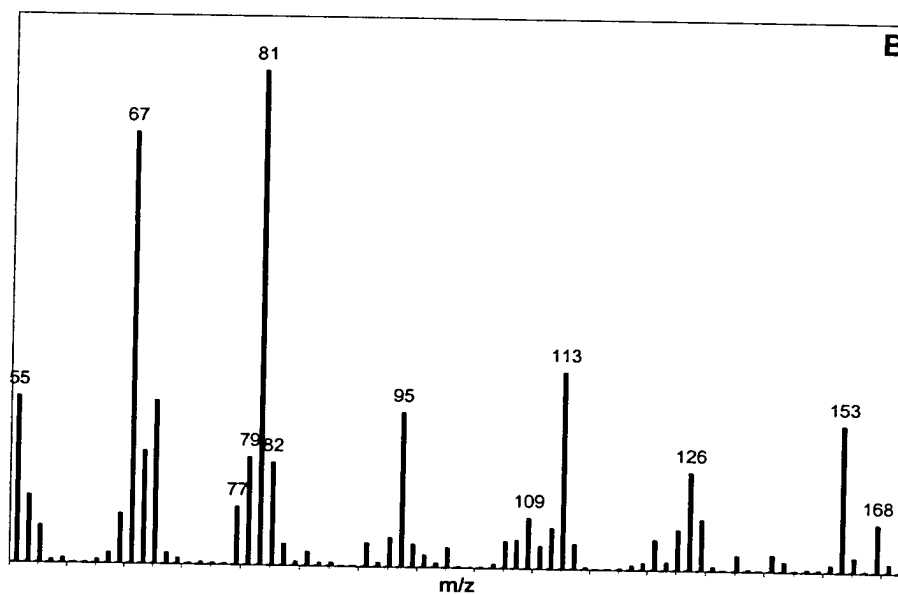
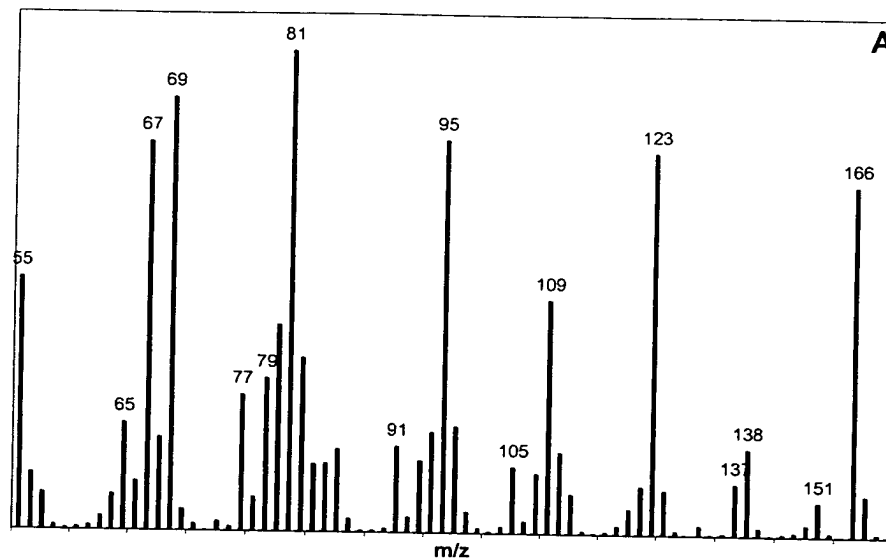


Figure 3 Mass spectra of nepetalactone (A) and dihydronepetalactone (B) peaks from GC-MS analysis.



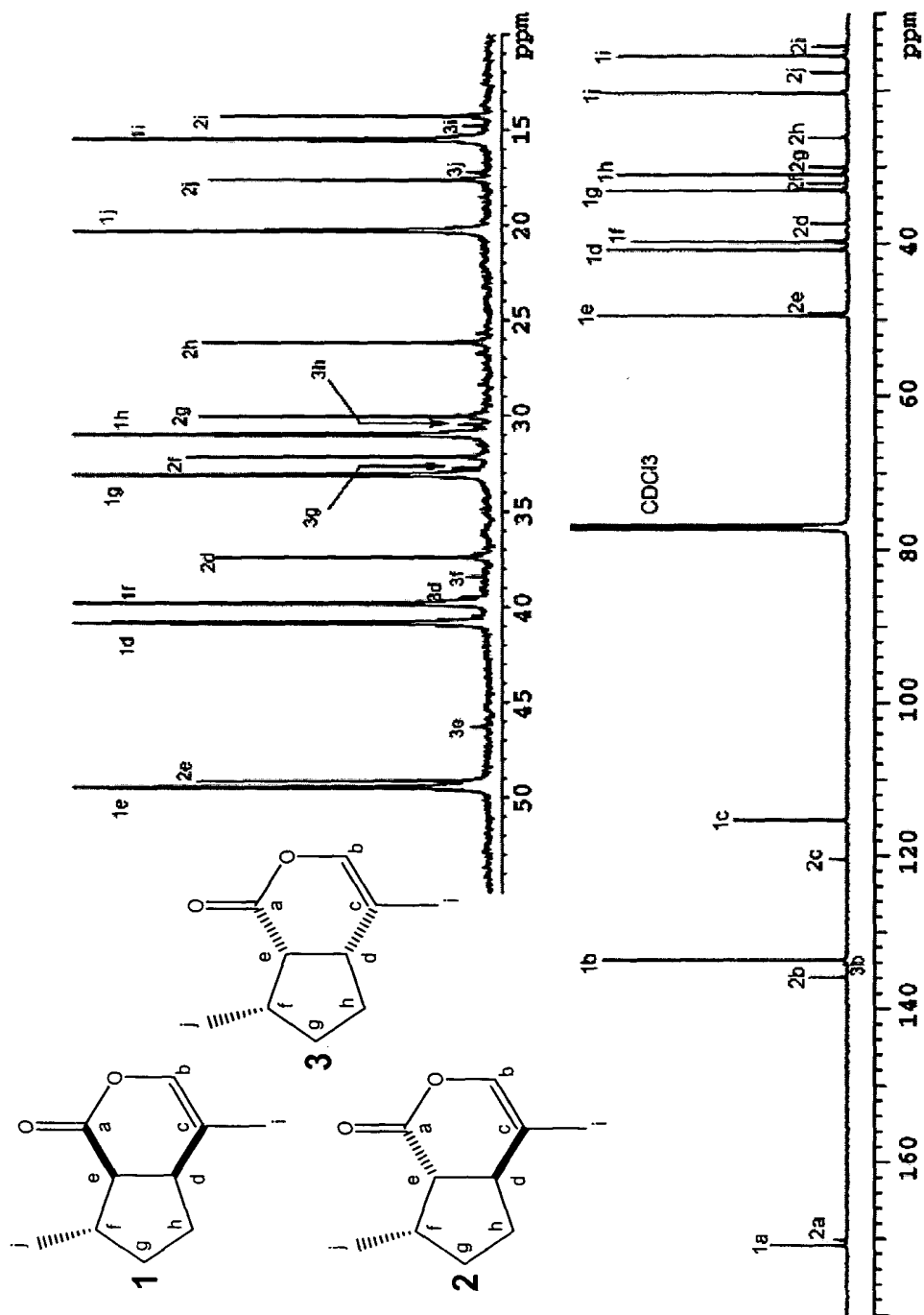


Figure 4 ¹³C NMR analysis of nepetalactones in fractionally-distilled catmint oil.

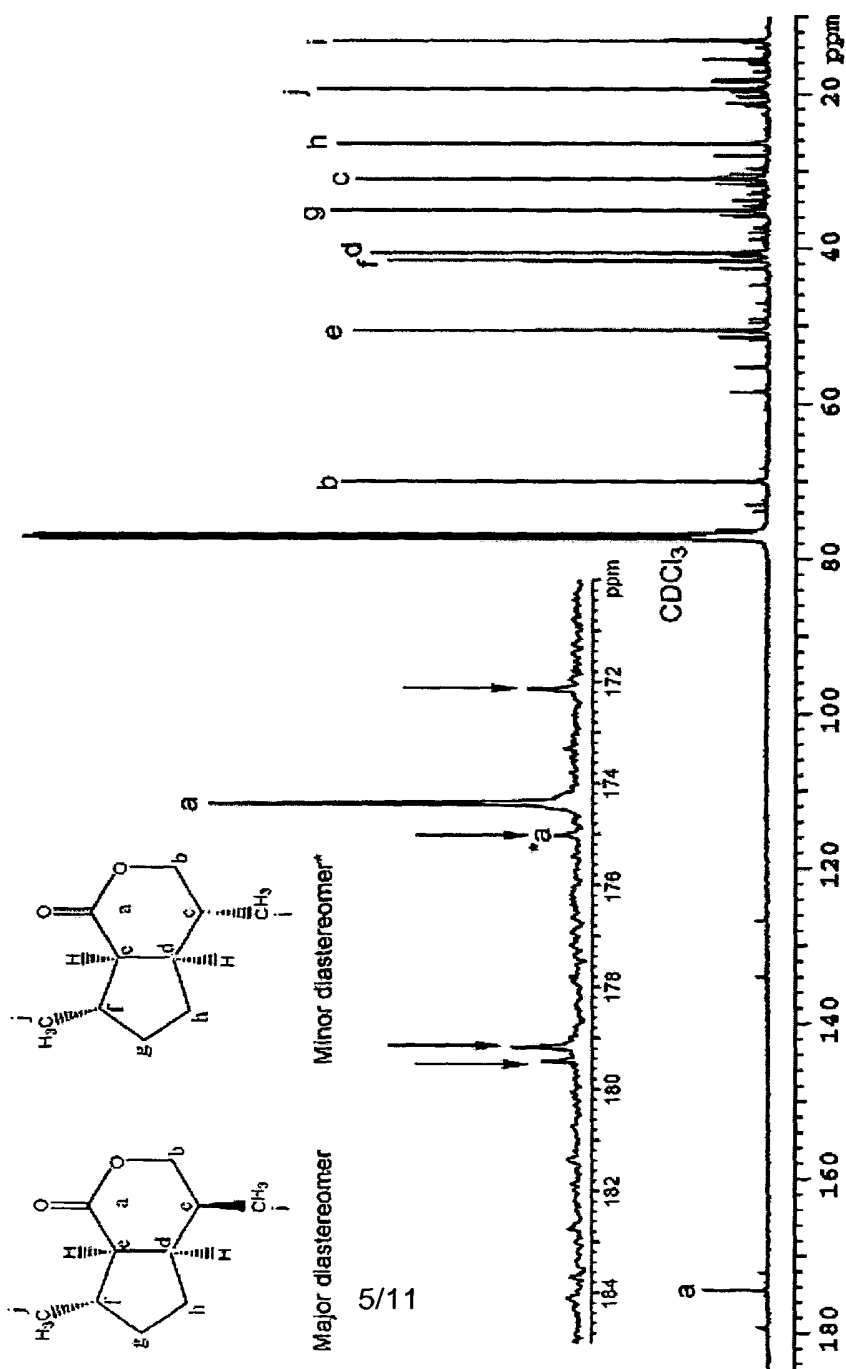


Figure 5 ^{13}C NMR analysis of dihydronepetalactones in hydrogenated catmint oil.

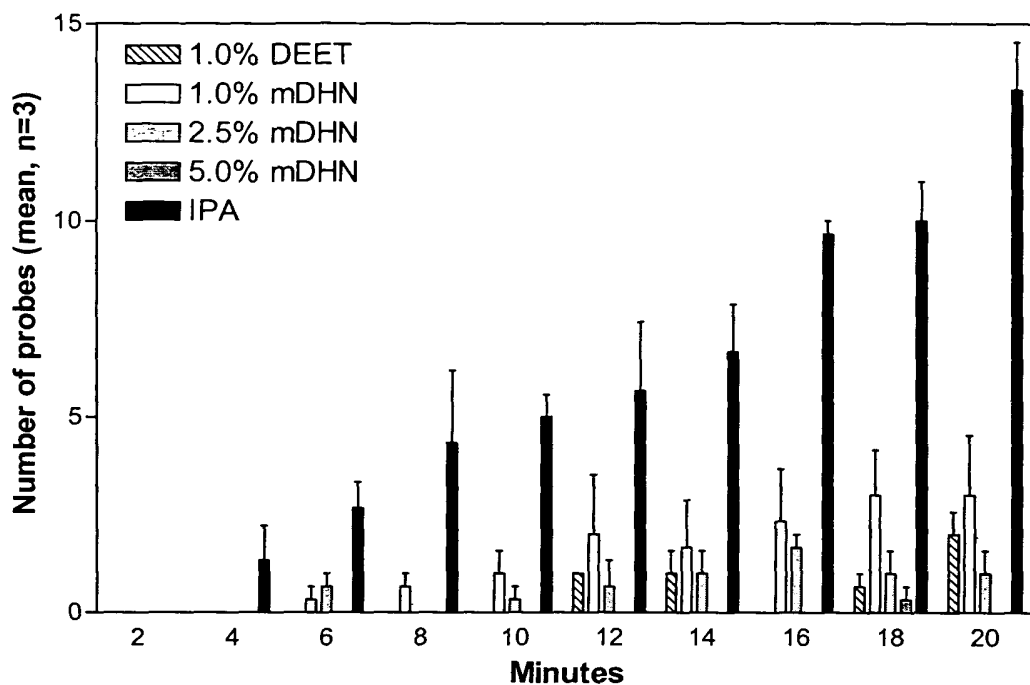


Figure 6 Distribution of probing density over time (*Aedes aegypti* mosquitoes; dihydronepetalactones derived from hydrogenation of a mixture of nepetalactone stereoisomers).

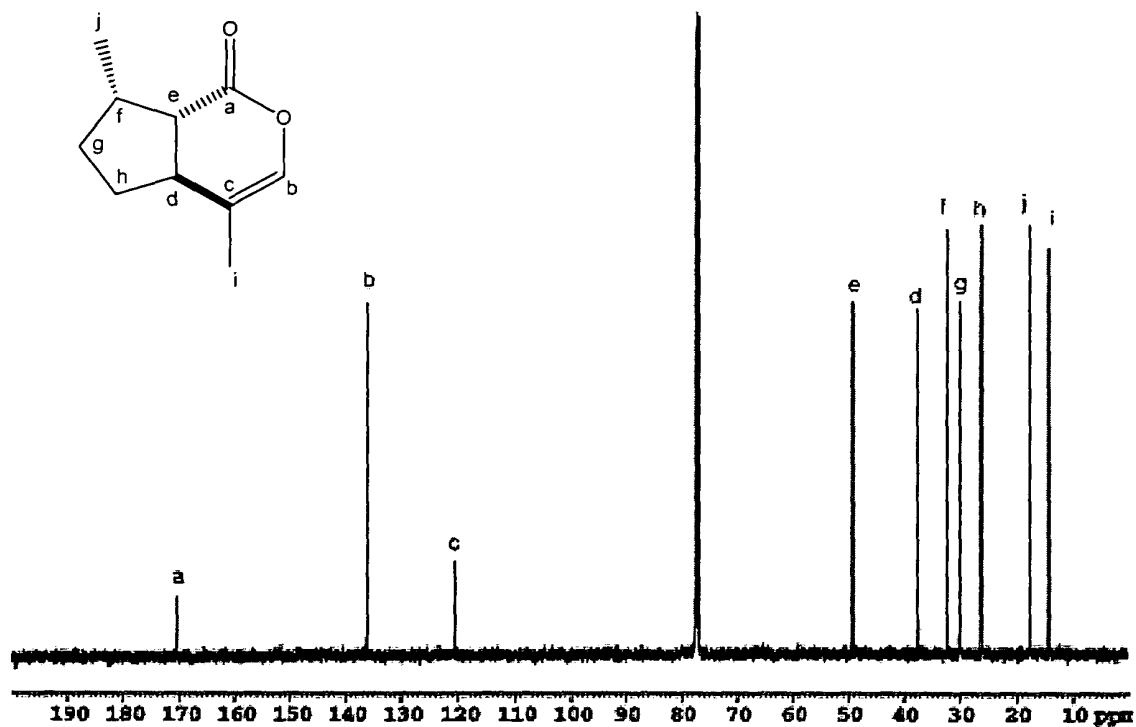


Figure 7 ¹³C NMR analysis of *trans,cis*-nepetalactone.

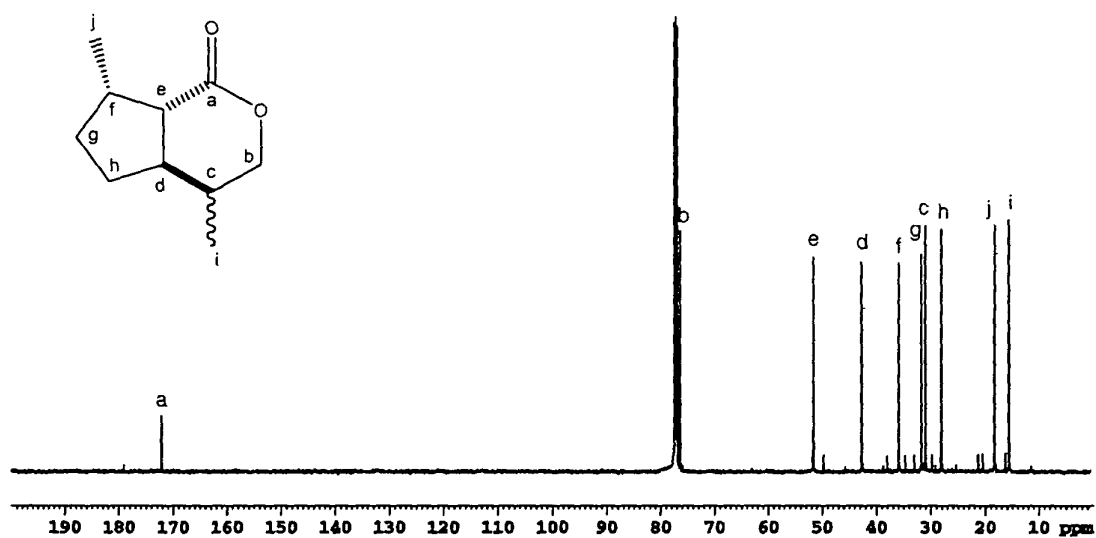


Figure 8 ^{13}C NMR analysis of dihydronepetalactones derived from hydrogenation of *trans*,*cis*-nepetalactone.

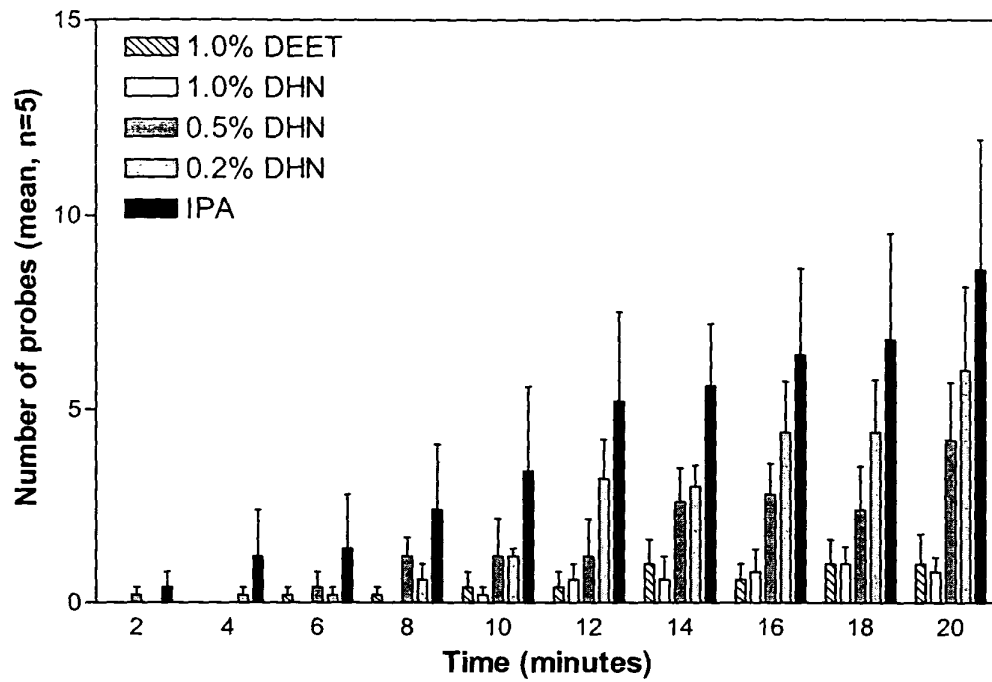


Figure 9 Distribution of probing density over time (*Aedes aegypti* mosquitoes; dihydronepetalactones derived from hydrogenation of *trans,cis*-nepetalactone).

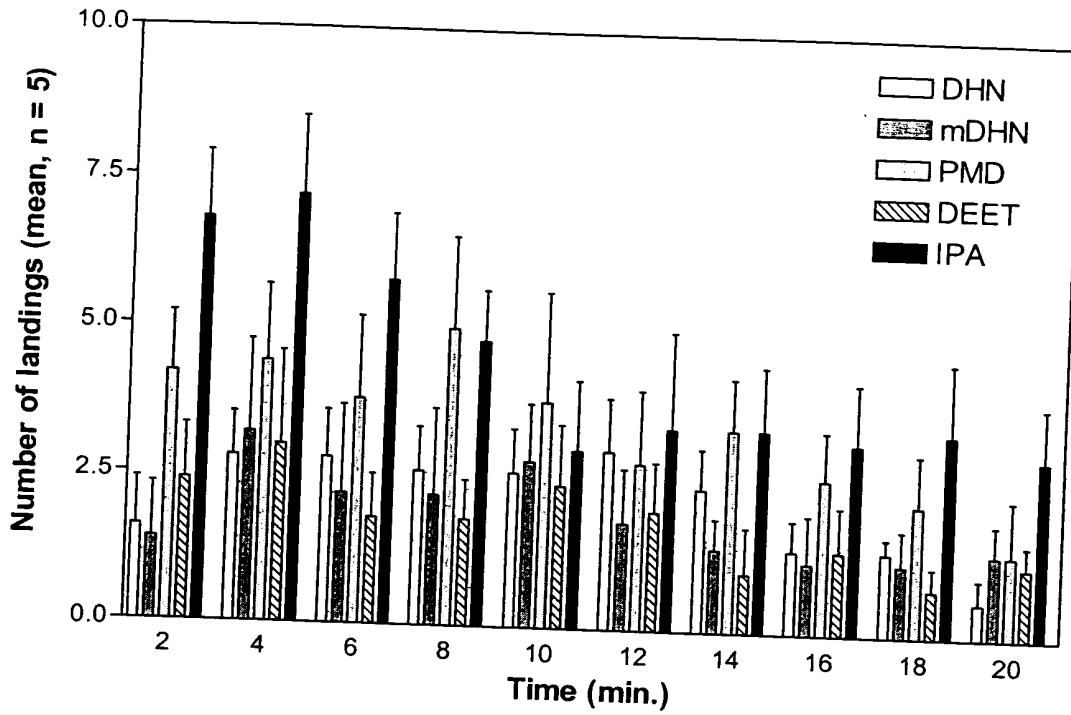


Fig. 10 Distribution of landing density with time, during tests of various repellents against stable flies (*Stomoxys calcitrans*).

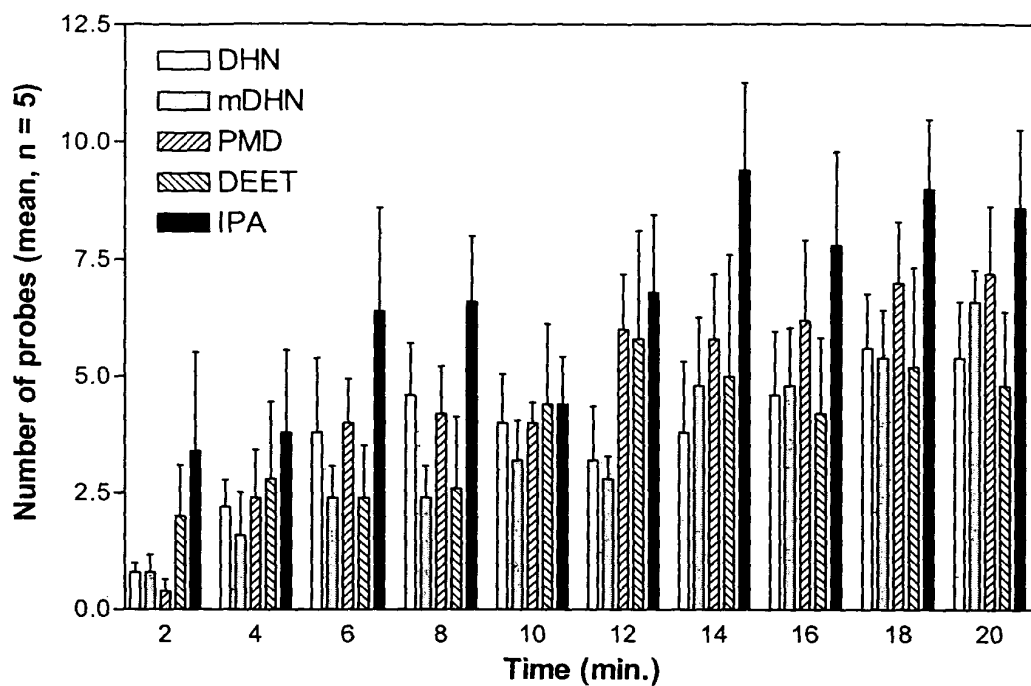


Fig. 11 Distribution of probing density with time, during tests of various repellents against anopheles mosquitoes (*A. albimanus*).